Precision polarization measurements of atoms in a far-off-resonance optical dipole trap

F. Fang, D. J. Vieira, and X. Zhao*
Los Alamos National Laboratory, Los Alamos, New Mexico 87545, USA
(Received 26 July 2010; published 31 January 2011)

Precision measurement of atomic and nuclear polarization is an essential step for beta-asymmetry measurement of radioactive atoms. In this paper, we report the polarization measurement of Rb atoms in an yttrium-aluminum-garnet (YAG) far-off-resonance optical dipole trap. We have prepared a cold cloud of polarized Rb atoms in the YAG dipole trap by optical pumping and achieved an initial nuclear polarization of up to 97.2(5)%. The initial atom distribution in different Zeeman levels is measured by using a combination of microwave excitation, laser pushing, and atomic retrap techniques. The nuclear-spin polarization is further purified to 99.2(2)% in 10 s and maintained above 99% because the two-body collision loss rate between atoms in mixed spin states is greater than the one-body trap loss rate. Systematic effects on the nuclear polarization, including the off-resonance Raman scattering, magnetic field gradient, and background gas collisions, are discussed.

DOI: 10.1103/PhysRevA.83.013416 PACS number(s): 37.10.−x, 32.80.Qk, 32.10.Bi, 21.10.Hw

I. INTRODUCTION

Optical trapping of radioactive atoms has great potential in undertaking precise measurements for testing fundamental physics, including electric dipole moment (EDM) measurement [1], atomic parity nonconservation (PNC) studies [2], β-recoil measurements of ^{38m,37}K ($t_{1/2} = 0.9$ s) [3,4] and ^{21}Na ($t_{1/2} = 21$ s) [5] in a magneto-optical trap (MOT), and β asymmetry of ^{82}Rb ($t_{1/2} = 75$ s) in a time-average orbiting potential (TOP) magnetic trap [6] and in a far-off-resonance optical dipole trap (FORT) [7]. Radioactive atoms confined in a FORT are ideal samples for studying parity-violating β decay of spin-polarized nuclei with the potential of searching for new physics beyond the standard model, i.e., deviations from maximal parity violation in the weak force.

Despite the phenomenological success of the standard model, the fundamental origin of parity violation is still unknown. Nuclear β-decay experiments continue to serve as a probe of the origin of parity violation and, more generally, the helicity structure of the weak interaction [8]. The β-asymmetry measurement owing to parity violation was first demonstrated by Wu [9] in 1957. Over the years, preparation of a gas sample of polarized nuclei became easier with the development of optical pumping, enabling highly polarized samples and high statistical accuracy in the β-asymmetry measurement. Systematic errors arising from β-particle backscattering and the quantification of the sample polarization limit the accuracy of the measurement to the 1% level.

Precision measurement of the spin polarization of atomic beams has been demonstrated for a Cs PNC measurement [10], but has yet to be shown for trapped atoms despite a few claims that high polarization was achieved. A variety of traps were considered for β-asymmetry measurements, including those that can selectively trap atoms in specific Zeeman states (i.e., near-resonance optical traps) [11] and TOP magnetic trap. However, the TOP trap suffers from systematic errors caused by the finite size of the atomic cloud in the trap and the magnetic-field gradient necessary for atom trapping. Evaporative or sympathetic cooling would mitigate this problem but at the expense of substantial atom loss and therefore are not suitable for β-asymmetry measurements with radioactive atoms. In a near-resonance optical dipole trap, a state-dependent trapping potential helps to achieve high polarization, but the trap lifetime is short owing to the relatively large off-resonance scattering rate.

For such polarization studies we previously used a FORT and already demonstrated the trapping of radioactive ^{82}Rb with a trap lifetime of more than 50 s [7], which is comparable to the half-life of ^{82}Rb. In this paper, we report on the realization of highly polarized ensembles of Rb atoms confined in an yttrium-aluminum-garnet (YAG) FORT and the precise measurement of atomic and nuclear polarization. We have prepared a cold cloud of polarized atoms in the YAG dipole trap by optical pumping to obtain an initial polarization of up to 97.2(5)%. The sample polarization is further purified to 99.2(2)% and maintained at that level when the two-body collision loss rate between atoms in different spin states is greater than the one-body trap loss [12]. We also tested that a rotating bias field has no measurable effect on the atomic polarization in the FORT, enabling a complete mapping of the β-$\vec{J}$ angular distribution for a β-asymmetry measurement.

II. EXPERIMENT

We use the same double-MOT system that was previously described in detail for trapping radioactive ^{82}Rb atoms [7]. The current measurements were all done using ^{85}Rb as a test bed for the method. Atoms collected in the first MOT (MOT1) are pushed to a scientific chamber a meter away by a laser beam and collected in a second MOT (MOT2), which has a pressure of better than 10^{-11} Torr and a typical pressure-limited trap lifetime of ∼100 s. The atoms trapped in MOT2 are then loaded in a YAG laser FORT (∼30 μm, $1/e$ diameter) with a wavelength of $\lambda = 1030$ nm and a typical power of ∼1.6 W. The typical dipole trap loading efficiency is ∼4% in this work. A schematic of the apparatus is shown in Fig. 1.

To polarize the atoms into the stretched upper hyperfine state ($5S_{1/2}, F = 3, m_F = 3$), an optical pumping pulse is applied once atoms are loaded in the FORT. Optical pumping (OP) and repump (RP) lasers are σ^+ light (circularly polarized

*xxz@lanl.gov

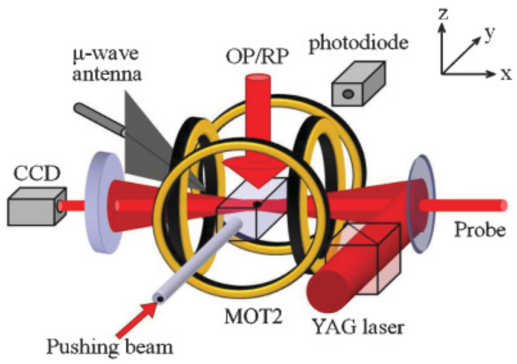

FIG. 1. (Color) The schematic of the experimental setup (not in scale, the MOT2 setup is on a 3×3 ft^2 breadboard). Atoms are transferred to MOT2 and loaded into a YAG FORT. An optical pump and repump pulse (OP/RP) is applied to polarize the atoms to the stretched state, and the atomic distribution in different m$_F$ states are measured using resolved microwave and optical transitions. Atomic and nuclear polarization are derived from these measurements.

to better than 99%) on resonance with $F = 3 \rightarrow F' = 3$ and $F = 2 \rightarrow F' = 3$ transitions for ^{85}Rb with typical powers of 40 μW and 2 mW, respectively. To drive the hyperfine transitions for measuring the m_F state populations, a microwave antenna is used (Sunol Sciences Corp. LP60) with a frequency range of 1.3–6.0 GHz, which covers the hyperfine transitions for both ^{85}Rb and ^{82}Rb isotopes. The antenna is positioned ∼5 cm from the trap with a typical input power of 1 W. To calibrate the absolute number of atoms in the dipole trap, we perform absorption imaging of the atoms. A probing beam on resonance with the $(F = 3,m_F = 3) \rightarrow (F' = 4,m_F = 4)$ transition propagates along the FORT beam axis and the absorption image is focused on a CCD camera. The OP and trap lasers have a linewidth of 0.5 and 1 MHz, respectively. The number of atoms in the FORT is typically 10^5 for this work, approximately the same as what we expect for a ^{82}Rb β-asymmetry experiment in the future.

To measure the number of atoms in the stretched state, we use resolved Zeeman spectroscopy by applying a bias field of 90 G and shifting the probe beam by 126 MHz. To measure the relative population in the stretched state respect to the total number of atoms, a 0.5-ms probe beam pulse on resonance with the $(F = 3,m_F = 3) \rightarrow (F' = 4,m_F = 4)$ transition pushes away the atoms in the stretched state $(F = 3,m_F = 3)$. Then MOT2 is turned on 20 ms after the push, and the fluorescence signal of the recaptured atoms is collected by using a photodiode. We measured both the retrap signals with and without the push beam to get the ratio of the atoms in the stretched state.

An optical approach alone is not enough to determine the population distribution in the nonstretched spin states owing to the lack of cycling transitions to the $5P_{3/2}$ states. We therefore use resolved microwave transitions with a bias field of 1 G for the spin state distribution measurement. To measure the atom distribution in the $F = 3$ states after optical pumping, a microwave pulse was applied to transfer atoms from a specific $(F = 3,m_F)$ state to the $F = 2$ level, after which a push beam was applied to push away atoms in the $F = 3$ states. The atoms shelved in the $F = 2$ state are recaptured in MOT2, and the retrap signal is used to measure the number of atoms transferred. Please note that this relative measurement of popuation distribution can be done with much higher precision than the absorption imaging measurement for the absolute number of atoms, and enables a precise measurement of the polarization.

III. MEASUREMENT, RESULTS, AND DISCUSSION

A. Optical pumping the atoms to the stretched state

For β-asymmetry measurements in a FORT, it is advantageous to have high atomic and nuclear polarization that would have a longer trapping lifetime owing to the lower two-body collision loss rate [7] and maximal asymmetry amplitude. To achieve high atomic and nuclear polarization, the polarization of the OP and RP lasers, bias field uniformity, and the overlap of the laser beams with the bias field have to be optimized. These optimizations were accomplished by optimizing the number of atoms that remain trapped after exposure to a prolonged optical pumping beam at high power. When these parameters are not optimal, the atoms are accelerated and pushed out of the trap by the pumping beam. When the optimal optical pumping condition is reached, the atoms fall into the dark stretched state $(F = 3,m_F = 3)$ after a few photon scattering events and remain in the trap. The number of atoms that remain in the FORT are measured by recapturing them in MOT2 and monitoring the fluorescence (retrap signal). We used a prolonged optical pumping pulse duration of 30 ms with 0.5-mW power for both OP and RP beams and a beam diameter of 3 mm. The dependence of optical pumping efficiency on the OP and RP laser polarizations (wave-plate setting) and the residual bias magnetic fields $\Delta B_x, \Delta B_y$ are shown in Figs. 2(a) and 2(b), respectively.

From these measurements, we optimize the alignment of the bias magnetic field with the OP and RP laser beams to $\Delta B_{x,y}$ of less than 1.5% of B_z, and set the $\lambda/4$ wave plate for the OP and RP lasers within 1° for σ^+ polarization. Calculations of the atomic population distribution owing to the residual σ^- and π polarization in the optical pumping beam are shown in Figs. 2(c) and 2(d), respectively. Once the bias field and laser polarization were optimized, the power of the OP beam is reduced to 40 μW, while the power of the RP beam was increased to 2 mW. This OP and RP pumping pulse is applied for 5 ms once the atoms are loaded in the FORT and the atoms are polarized largely in the stretched state $(F = 3,m_F = 3)$ for ^{85}Rb. In this case, the atoms in the lower hyperfine level are calculated to be negligibly small, as shown in Figs. 2(c) and 2(d). This also was confirmed with a push and recapture measurement.

B. Measurement of m$_F$ state population distribution

It is straightforward to prepare atoms in the same hyperfine level by controlling the timing and power of the repump laser pulse during loading. As mentioned earlier, once the atoms are in the desired hyperfine level, we measure the m_F state distribution by using a microwave pulse to transfer the atoms from a particular m_F state to a different hyperfine level, and then use a laser pulse to either image or push out the remaining atoms for a population measurement.

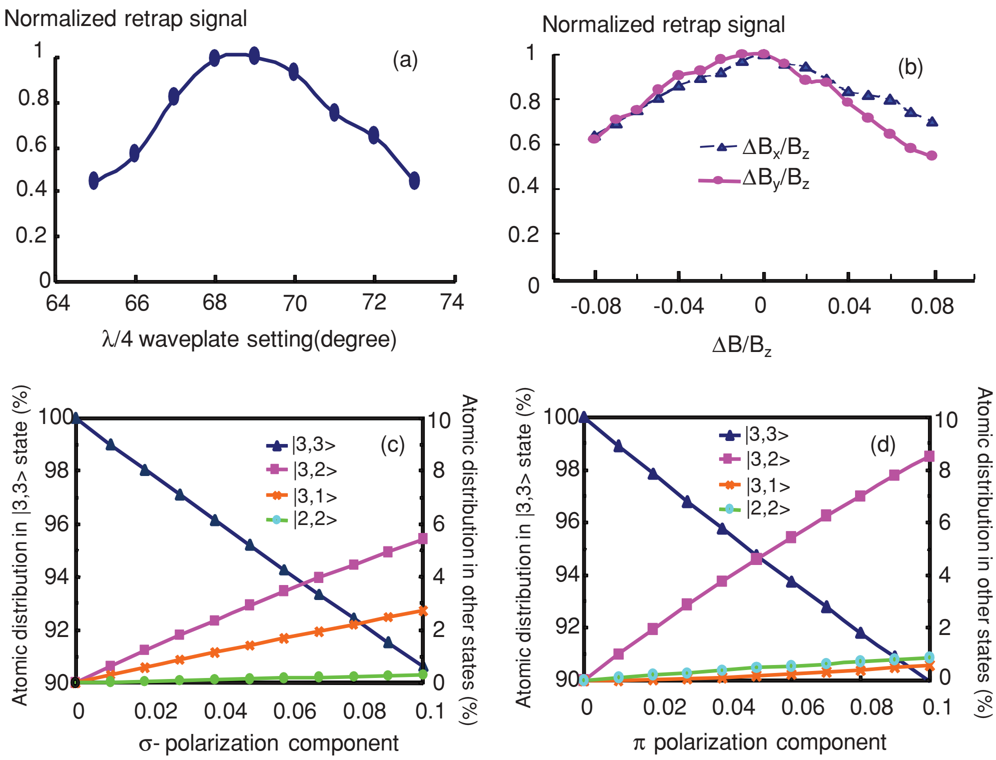

FIG. 2. (Color) Dependence of optical pumping on the polarization of the OP and RP lasers and bias magnetic field. (a) Retrap signal vs $\lambda/4$ wave-plate setting. When the retrap signal is high, the atoms are pumped into the dark stretched state. Imperfections in the polarization of the light will induce σ^- transitions and reduce the polarization of the sample. (b) Retrap signal vs residual B field in the x and y direction. The residual magnetic field in these directions will induce π transitions and reduce the polarization of the sample. The magnetic-field alignment is better than 1% in both directions, which gives an alignment of better than 1.5% overall. (c) Theoretical calculations of the distribution of different atomic Zeeman states as a function of residual σ^- component. (d) Theoretical calculations of the distribution of different atomic Zeeman states as a function of residual π component.

Because the microwave transitions have different linewidths owing to the magnetic-field broadening, the efficiency of the microwave pulses for population transfer vary for different transitions [10]. We first tested out this technique with unpolarized atoms to compare the transfer efficiency for the different transitions. We prepare an unpolarized sample of atoms in the lower hyperfine $F = 2$ level by applying an optical depumping beam to the trapped atoms. A microwave pulse on resonance with $(F = 2, m_F) \rightarrow (F = 3, m_F)$ transitions subsequently pumps the atoms to the $(F = 3, m_F)$ state under a 1-G bias magnetic field. An absorption image is then taken to measure the atoms transferred to the upper $F = 3$ states. We were able to observe Rabi oscillations between $(F = 2, m_F = 0)$ and $(F = 3, m_F = 0)$ states with a microwave pulse duration of 0.35 ms. We did not observe Rabi oscillations for other π transitions and instead used a pulse of 5-ms duration to saturate the transition. We also observed Rabi oscillations between $(F = 2, m_F = 2)$ and $(F = 3, m_F = 3)$ states with a microwave pulse duration of 50 μs.

We can compare the transfer efficiency between a Rabi π pulse and a microwave saturation pulse by applying either pulse to the atoms in the same state $(F = 2, m_F = 2)$. A Rabi π pulse drives the $(F = 2, m_F = 2) \rightarrow (F = 3, m_F = 3)$ transition while the saturation pulse drives $(F = 2, m_F = 2) \rightarrow (F = 3, m_F = 2)$ to saturation. The ratio between the number of atoms transferred into the $F = 3$ level by these two microwave pulses is 1.7. Figure 3(a) shows the Rabi oscillation of the transition $(F = 2, m_F = 2) \rightarrow (F = 3, m_F = 3)$, where the the signal decay is owing to the residual bias field gradient. Figure 3(b) shows the distribution of the number of atoms transferred by the microwave pulses, which is consistent with a uniform distribution for an unpolarized sample. The $(F = 2, m_F = 0)$ state has a better transfer rate because a Rabi π pulse is applied. From these measurements we conclude that the atoms are uniformly distributed among the $F = 2$ Zeeman sublevels without optical pumping, and the efficiency of a Rabi π pulse and a microwave saturation pulse are 85% and 50%, respectively.

Utilizing the combination of microwave drive and the push and retrap technique mentioned earlier, we are able to measure the population distribution in the $F = 3$ Zeeman states. These results are shown in Table I.

From Table I, we can see that most of the atoms are in the stretched state after optical pumping. The percentage of atoms in the nonstretched states are consistent with the imperfection in the bias field and laser polarization as shown in Fig. 2. The measurement method has a systematic error owing to off-resonant scattering from the push beam, because it excites a small fraction of atoms to the $(5P_{3/2}, F' = 3)$ state that eventually decay back to the $(5S_{1/2}, F = 2)$ state and remain in the trap. To measure the systematic error, atoms are pumped into the upper hyperfine $F = 3$ level with the repumping beam,

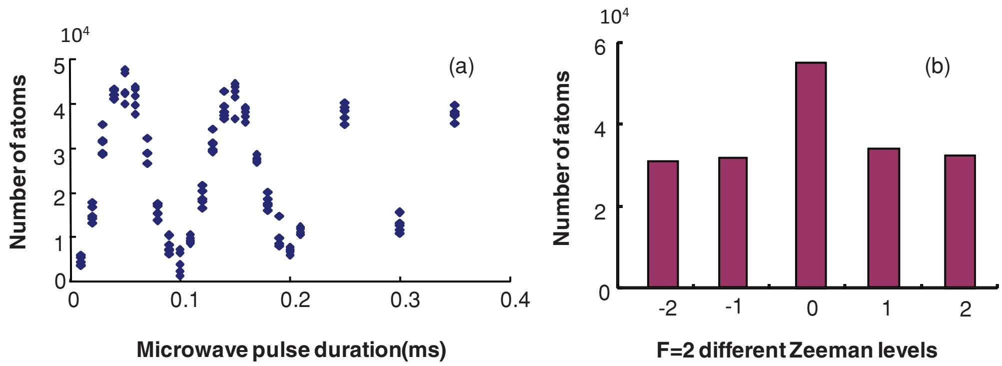

FIG. 3. (Color online) Microwave transition and transfer efficiency of different microwave transitions. (a) Rabi oscillation of the transition $(F = 2, m_F = 2) \rightarrow (F = 3, m_F = 3)$ with a relaxation time of ~0.7 ms owing to the residue magnetic field gradient. (b) State distribution without optical pumping. $(F = 2, m_F = 0) \rightarrow (F = 3, m_F = 0)$ was measured with a Rabi π pulse. Other states are measured with a microwave duration of 5 ms.

and then a pushing pulse on resonance with $F = 3 \rightarrow F' = 4$ is applied without any bias magnetic field, so all atoms in the $F = 3$ level are in resonance with the push light. The percentage of atoms remaining in the trap is measured as a function of pushing laser power, and the result is shown in Fig. 4.

We observe that even with a pushing beam power of less than 3 μW (0.4 mW/cm^2), 1% of the atoms are still recaptured. This systematic error has been corrected in Table I above. Other systematic effects are much smaller and discussed later.

C. Polarization evolution in the dipole trap and nuclear polarization

With a trap lifetime of 50 s for atoms optically pumped to the stretched $(F = 3, m_F = 3)$ state, the atomic polarization further purifies owing to hyperfine changing collisions. Collisions between atoms in different spin states lead to a loss of atoms from the trap and therefore an increase in the relative population of the (3, 3) states. This population evolution was measured as a function of trapping time as shown in Fig. 5. It shows that the fraction of atoms in the stretched (3,3) state increases to 98% (corresponding to a polarization of 99%) in the first 10 s.

For β-asymmetry measurement, we need to know the nuclear polarization. The nuclear spin for different Zeeman levels is shown in Fig. 6(a) and the calculated nuclear-spin evolution from the m_F state population measurement in the first 10 s is shown in Fig. 6(b). Nuclear polarization was calculated as

$$\langle P_I \rangle = (n_3 - n_{-3}) + \tfrac{2}{3}(n_2 - n_{-2}) + \tfrac{1}{3}(n_1 - n_{-1}) \quad (1)$$

$$= 1 - \tfrac{1}{3}(n_2 + 2n_1 + 3n_0 + 4n_{-1} + 5n_{-2} + 6n_{-3}), \quad (2)$$

where $\langle P_I \rangle$ is the nuclear polarization for atoms in the $F = 3$ states, and n_{m_F} is the fraction of atomic population in the $(F = 3, m_F)$ state. We use the second equation to calculate the polarization, which yields smaller statistical error when n_3 closes to 1.

TABLE I. Atomic population of (F, m_F) after optical pumping. The power of the optical pumping and repump beams are 40 μW and 2 mW, respectively, with a beam diameter of 3 mm. An optical pumping pulse with a duration of 5 ms was applied once the atoms are loaded in the dipole trap.

States (F, m_F)	Fraction of atomic population (error)
3,3	0.947 (0.038)
3,2	0.041 (0.004)
3,1	0.008 (0.003)
3,0	0.001 (0.002)
2,2	$\leqslant$0.001
Other states	$\leqslant$0.001

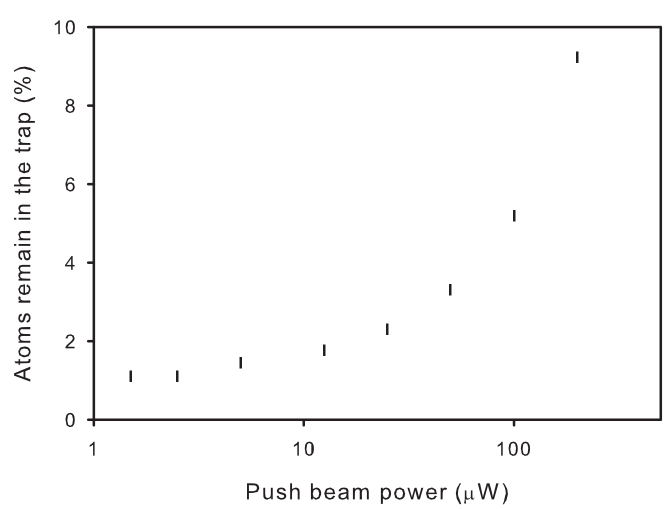

FIG. 4. Measurement of the number of atoms remaining in the trap as a function of the pushing beam power. Trapped atoms are prepared in the $F = 3$ hyperfine level, then a pushing beam on resonance with the $F = 3 \rightarrow F' = 4$ transition under minimal bias field is applied to push atoms away. After waiting for 20 ms, MOT2 is turned on to recapture the remaining atoms and the retrap signal is measured with a photodiode. When the pushing beam power is high, some of the atoms end up in the $F = 2$ hyperfine level owing to off-resonant transitions, and are recaptured in the trap. This effect is small at low push beam power (~1% at 3 μW).

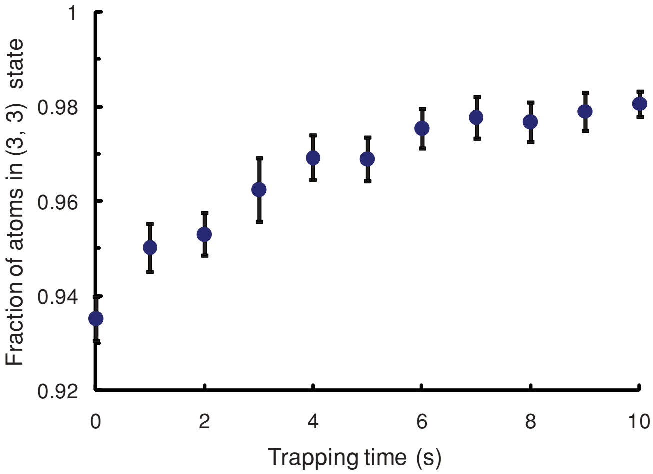

FIG. 5. (Color online) Fraction of atomic populations in the $(F=3,m_F=3)$ state at different trap holding times. The relative population signals are measured with the pushing and retrap method. After optical pumping, atoms are held in the FORT for a variable time. Then, a 2-μW pushing beam on resonance with the $(F=3, m_F=3)\rightarrow(F'=4,m_{F'}=4)$ transition under 90-G bias field is applied to clean up the atoms in the $(F=3,m_F=3)$ states. MOT2 is back on 20 ms later to recapture and measure the remaining atoms. The relative population in the $(F=3,m_F=3)$ state is derived by comparing the retrap signal with and without the push beam. The systematic error mentioned earlier has been corrected.

D. Off-resonance Raman scattering

Off-resonant Raman scattering owing to the FORT YAG laser could potentially depolarize the atoms after the atomic polarization was purified to 99% in the first 10 s. In our experiment, the trap laser is linearly polarized with trap depth of 250 μK and a scattering rate of 3 Hz [12]. The off-resonance Raman scattering rate [14] is

$$\Gamma_{\mathrm{Ra}}=\frac{3\pi c^2\omega_L^3 I}{2h\mu^4}\left[\frac{\alpha^{(1/2)}_{FM\rightarrow F'M'}}{\Delta_{1/2}}+\frac{\alpha^{(3/2)}_{FM\rightarrow F'M'}}{\Delta_{3/2}}\right]^2, \qquad (3)$$

where Γ_{Ra} is the off-resonant Raman scattering owing to the YAG laser, $\alpha^{J'}_{FM\rightarrow F'M'}/\Delta_{J'}$ are the amplitudes for a spontaneous scattering path through intermediate states within the $5P_{J'}$ levels, $\omega_L=2\pi c/\lambda$ is the FORT laser frequency, and I is its intensity. We estimate that Γ_{Ra} is $\sim$3 mHz in our case. The evolutions of the atomic number in different spin states follow these equations [12]:

$$\frac{dn_s}{dt}=-\frac{n_s}{\tau}-\beta_2' n_s^2-\beta_2 n_s n_n-n_s\Gamma_{\mathrm{Ra}}, \qquad (4)$$

$$\frac{dn_n}{dt}=-\frac{n_n}{\tau}-\beta_2 n n_n+n_s\Gamma_{\mathrm{Ra}}, \qquad (5)$$

where n_s,n_n,n are the density of atoms in the stretched, nonstretched, and all states, respectively; β_2',β_2 are the two-body collision loss rates for the stretched (owing to evaporative cooling) and hyperfine changing collisions, respectively; and τ is the background pressure-limited lifetime. A theoretical calculation of the evolution of the spin polarization in the trap is shown in Fig. 7. We can see that off-resonant Raman scattering is not a problem. Moreover, this effect can be suppressed further by using circularly polarized trapping light. Because the polarization evolution depends on the collisions between the trapped atoms, the ultimate polarization achieved may vary from species to species.

E. Other systematic issues in the polarization measurement

Magnetic-field gradients will give a systematic error when the atomic cloud spreads out in size. This is a big problem when using a TOP trap owing to the large field gradients required for trapping. In our experiment, we use a FORT and apply a uniform rotating magnetic field of 90 G. The atomic cloud size is 30 μm in the trap radial direction and 200 μm in the longitudinal direction. The residual magnetic field is less than 10 mG, giving $\frac{\Delta B_\perp}{B_0}\ll 0.001$, which gives a systematic error of less than 0.1% in the final polarization measurement. There are also field gradients arising from the coils that produce the rotating magnetic field. The coils are two pairs of Helmholtz coils with the coil diameters of 10 cm. The largest field inhomogeneity is $\leqslant$0.2% at 0.1 mm away from

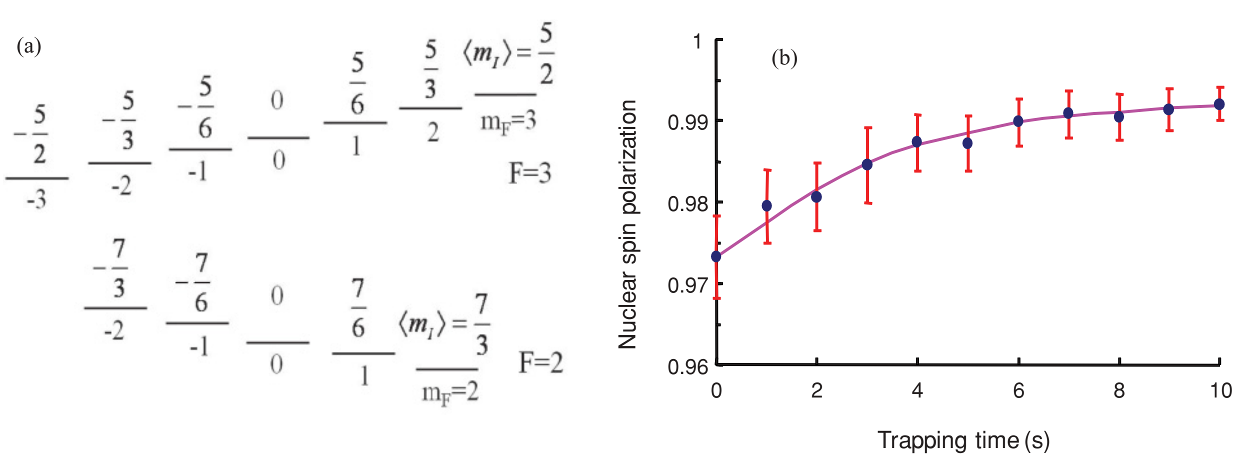

FIG. 6. (Color online) Nuclear-spin evolution in the FORT. (a) Nuclear spin for different Zeeman levels. (b) Nuclear polarization evolution in the FORT for the first 10 s. Nuclear polarization was calculated using the measurement of the population distribution and the average nuclear spin of each m_F state.

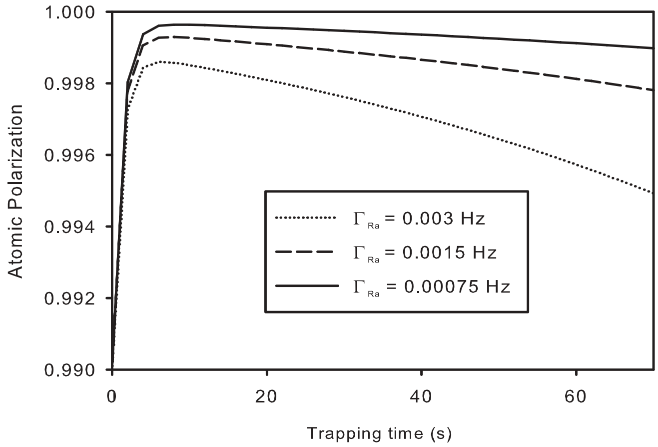

FIG. 7. Theoretical calculations of the nuclear-spin evolution in the FORT owing to both trap light Raman scattering and two-body collisions.

the center, which gives the systematic error of less than 0.2%. Another source of error comes from polarization changing collisions with the background gas. At a vacuum of less than 10^{-11} Torr, these errors are negligible.

IV. SUMMARY

In summary, we have prepared highly polarized atoms and demonstrated the precise measurement of the sample polarization to better than the 1% level. We have also studied the time evolution of the polarization in a YAG FORT. We have prepared cold clouds of polarized atoms with a polarization of up to 97.2(5)% by carefully optimizing the optical pumping process in the YAG FORT. The spin polarization of these trapped atoms is further purified to 99.2(2)% and maintained at this level by cold atom collisions when the two-body collision loss rate between atoms in mixed spin states is greater than the one-body trap loss rate. The improved polarization measurement accuracy was achieved by detailed mapping of the atomic populations in the Zeeman sublevels by using resolved microwave and optical Zeeman spectroscopy. The effects on the nuclear-spin polarization owing to the off-resonance Raman scattering and the residual magnetic field gradient are discussed. These advancements are an important step toward a new generation of precision measurements involving polarized trapped atoms. For a β-asymmetry experiment we plan to load ^{82}Rb from the primary MOT directly into the FORT, and transport the atoms to a scientific chamber in a few seconds to minimize the atom loss to the wall. After the atomic ensemble is fully polarized, a rotating magnetic field will be applied so that a complete mapping of the β-$\vec{J}$ angular distribution can be measured with a single β detector collimated to the trapped atoms.

ACKNOWLEDGMENTS

We thank Professor David Weiss, Dr. Y. Natali Martinez de Escobar, and Dr. Andrew Hime for helpful discussions related to spin polarization and β-asymmetry measurement. This work is supported by the Laboratory Directed Research and Development program at Los Alamos National Laboratory, operated by the Los Alamos National Security, LLC for the National Nuclear Security Agency (NNSA) as part of the US Department of Energy under Contract No. DE-AC52-06NA25396.

[1] J. R. Guest, N. D. Scielzo, I. Ahmad, K. Bailey, J. P. Greene, R. J. Holt, Z.-T. Lu, T. P. O'Connor, and D. H. Potterveld, Phys. Rev. Lett. **98**, 093001 (2007).

[2] S. Aubin, E. Gomez, L. A. Orozco, and G. D. Sprouse, Phys. Rev. A **70**, 042504 (2004).

[3] A. Gorelov *et al.*, Phys. Rev. Lett. **94**, 142501 (2005).

[4] D. Melconian *et al.*, Phys. Lett. B **649**, 370 (2007).

[5] P. A. Vetter, J. R. Abo-Shaeer, S. J. Freedman, and R. Maruyama, Phys. Rev. C **77**, 035502 (2008).

[6] S. G. Crane, S. J. Brice, A. Goldschmidt, R. Guckert, A. Hime, J. J. Kitten, D. J. Vieira, and X. Zhao, Phys. Rev. Lett. **86**, 2967 (2001).

[7] D. Feldbaum, H. Wang, J. Weinstein, D. Vieira, and X. Zhao, Phys. Rev. A **76**, R051402 (2007).

[8] J. Deutsch and P. Quin, in *Precision Tests of the Standard Electroweak Model*, edited by P. Langacker, World Scientific Advanced Series on Directions in High Energy Physics (World Scientific, Singapore, 1995).

[9] C. S. Wu *et al.*, Phys. Rev. **105**, 1413 (1957).

[10] B. P. Masterson, C. Tanner, H. Patrick, and C. E. Wieman, Phys. Rev. A **47**, 2139 (1993).

[11] K. L. Corwin, S. J. M. Kuppens, D. Cho, and C. E. Wieman, Phys. Rev. Lett. **83**, 1311 (1999).

[12] F. Fang, H. Wang, D. Feldbaum, D. J. Vieira, and X. Zhao, Phys. Rev. A **79**, 043406 (2009).

[13] N. Severijns *et al.*, Rev. Mod. Phys. **78**, 991 (2006).

[14] R. A. Cline *et al.*, Opt. Lett. **19**, 207 (1994).